This is the peer-reviewed, authors' version of the article:

M. Gruden, M. Zlatar, What is the nature of bonding in $[Fe(CO)_3(NO)]^-$ and $[Fe(CO)_4]^{2-}$?, Theoretical Chemistry Accounts, 2020, 139, 7, 126, doi: https://doi.org/10.1007/s00214-020-02639-3

What is the nature of bonding in $[Fe(CO)_3(NO)]^-$ and $[Fe(CO)_4]^{2-}$?

Maja Gruden[1,*] and Matija Zlatar[2,*]

[1] University of Belgrade - Faculty of Chemistry, Studentski trg 12-16, 11000 Belgrade, Serbia
e-mail: gmaja@chem.bg.ac.rs
ORCID: 0000-0002-0746-5754

[2] University of Belgrade – Institute of Chemistry, Technology and Metallurgy, National Institute, Njegoševa 12, 11000 Belgrade, Serbia
e-mail: matija.zlatar@ihtm.bg.ac.rs
ORCID: 0000-0002-3809-0940

* Corresponding authors: gmaja@chem.bg.ac.rs; matija.zlatar@ihtm.bg.ac.rs

Electronic supplementary material:

Energy Decomposition Analysis of $[Fe(CO)_3]^{2-}$-- CO at SR-ZORA-BP86-D4/TZP and SR-ZORA-BHandHLYP/TZP level of theory; Energy Decomposition Analysis of $[Fe(CO)_3$--$NO]^-$ for different fragmentation patterns at SR-ZORA-BP86-D4/TZP level of theory; Energy Decomposition Analysis of $[Fe(CO)_3$--$NO]^-$ for different fragmentation patterns, at SR-ZORA-BHandHLYP/TZP level of theory;

Acknowledgments

This work is supported by the Ministry of Education, Science, and Technological Development of the Republic of Serbia (Grants No. 451-03-68/2020-14/200168 and 451-03-68/2020-14/200026).

Abstract

To shed new light on the electronic structure of $[Fe(CO)_3(NO)]^-$ complex ion DFT based analysis of the nature of chemical bonding has been performed. For this purpose, the Extended Transition State Energy Decomposition Analysis alongside the Natural Orbital for Chemical Valence (EDA-NOCV) has been used and results compared to the nature and the strength of the interactions in isoelectronic $[Fe(CO)_4]^{2-}$ complex ion. Based on orbital contribution to the interaction energy and charge flow between the fragments, the ground state can be the best described as an open-shell singlet with zero formal oxidation state on iron and negative charge on the nitrosyl ligand. It is in agreement with the different nature of interactions when NO^+ and CO ligands are bonded to Fe(−II).

Keywords

Chemical bonding – Energy Decomposition Analysis – DFT – oxidation states – iron complexes

1. Introduction

In chemical compounds, iron can be found in various oxidation states (from -II to +VI) [1]. The most common ones are +II and +III, unusual oxidation states Fe(-II), Fe(-I), and Fe(0) have been found in organometallic compounds [1–4]. The $[Fe(CO)_3(NO)]^-$ has been the subject of interest in inorganic, organic, and physical chemistry, as well as in catalysis for many years [5–10]. Concerning its electronic structure, there is no general conclusion about the oxidation state of the central Fe atom and the resulting charge of the NO ligand, thus the determination of its ground electronic state. $[Fe(CO)_3(NO)]^-$ is isoelectronic with $[Fe(CO)_4]^{2-}$ with the oxidation state of the iron unambiguously accepted to be -II [11, 12]. Accordingly, iron in the first complex is expected to be in -II oxidation state. On the other hand, these two species have different catalytic activity in various organic reactions pointing into a difference in their electronic structure [5, 6, 8, 9]. The combined experimental and theoretical study proposed that the electronic structure of $[Fe(CO)_3(NO)]^-$ is best described as NO^- coordinated to Fe(0) [6]. More recent work gave different views on this subject more inline with the Fe(-II)-NO^+ bonding [7]. The vagueness of the nature of Fe-NO interaction in $[Fe(CO)_3(NO)]^-$ is a consequence of both the diversity of the electronic structures of transition metal complexes in general [13–16] and non-innocence of the nitric oxide type ligand [17–23]. Energies of iron 3d orbitals and π^* orbitals of NO are of comparable energies, complicating the determination of the oxidation state of iron as well as the nature of nitric oxide type ligand – NO^+, NO radical or NO^-.

In $[Fe(CO)_4]^{2-}$ iron is in a tetrahedral environment with formally d^{10} electronic configuration. All five molecular orbitals (MOs) with dominant d-character are completely filled, giving singlet as the ground state. Excellent π^*-accepting properties of the CO assist in the stability of the d^{10} complex. When the isoelectronic $[Fe(CO)_3(NO)]^-$ is considered in the same way, i.e., Fe(-II) and NO^+, naturally closed-shell singlet is again the ground state. In the other

situation, when there is an interaction between Fe(0) and NO^{-}, there are two unpaired electrons on the iron center (d^8 electronic configuration) and two unpaired electrons on nitrosyl anion. This leads either to the quintet or to the open-shell singlet state. Consequently, the nature of the bonding of nitrosyl ligand to the iron center must be different depending on the electronic structure. And the role of π^* orbitals of the nitric oxide is different.

The problem of the description of the electronic structure in $[Fe(CO)_3(NO)]^{-}$ is clearly multireference [6, 7]. Closed-shell singlet state and high-spin quintet state can be adequately described by one Slater determinant, but this is not the case for the open-shell singlet state. This instantly leads to the conclusion that multideterminantal methodologies that are based on configuration interaction should be used. Unfortunately, such methods did not give equivocal findings [6, 7]. Adequate treatment of the dynamical correlation is also necessary. As a single determinant method, conventional Kohn-Sham Density Functional Theory (KS-DFT) cannot rigorously describe multideterminantal states. Noodleman's suggestion was the approach called the broken-symmetry (BS), which represents multideterminantal states with only one „antiferromagnetically coupled" Slater determinant [13, 24–26]. Another drawback of all DFT-based methods is the dependence of the results on the choice of the Density Functional Approximations (DFA) employed. It is well known that the generalized gradient (GGA) functionals overestimate delocalization [27]. In contrast, hybrid functionals tend to localize electron, and the extent of the localization will be higher with a higher percentage of the exact Hartree-Fock (HF) exchange [28]. This situation occurs, e.g., in mixed-valence compounds [28], in homolytic dissociation [29, 30], charge transfer [31]. One of the solutions for this kind of problem is the use of long-range separated hybrid functionals [32, 33]. Alternatively, it is possible to tune the percentage of the exact exchange [28, 34], or to rely on some non-conventional DFT based methods like constrained DFT [35] or multiplet sum DFT method [36].

To shed new light on the problem of the electronic structure of $[Fe(CO)_3(NO)]^{-}$ we performed DFT bond analysis in the framework of Extended Transition State Energy Decomposition Analysis [37–39] with Natural Orbital for Chemical Valence (EDA-NOCV) method [40, 41] and compared it to the nature and the strength of the interactions in $[Fe(CO)_4]^{2-}$ complex ion. EDA based schemes have been proven to be compelling and trustworthy for understanding chemical bonding [39, 42–45].

2. Computational details

All calculations were done by DFT with the ADF program package (version 2019.302) [46–48]. The all-electron triple-zeta Slater-type orbitals plus one polarization function (TZP) basis set was used for all atoms. Relativistic effects were considered with the zeroth-order regular approximation to the Dirac Hamiltonian in the scalar-relativistic formulation (SR-ZORA) [49]. All calculations were performed on the complex ions from experimentally determined X-ray structures of $[Fe(CO)_3(NO)]^{-}$ (CCDC 1266312)[50] and $[Fe(CO)_4]^{2-}$ (CCDC 1217933)[11] with long-range separated hybrid CAMY-B3LYP [51–53]. Additionally, in

line with previously stated, to test the DFAs, 11 other functionals were used: GGAs in the form of BP86 [54–56] and OPBE [57]; meta-GGAs in the form of M06-L [58, 59], TPSS [60, 61], SCAN [62]; hybrid B3LYP* [63], B3LYP [64], BHandHLYP functionals and meta-hybrid M06 [58, 59], M06-2X [58, 59] and TPSSh [60, 61]. Hybrid and meta-hybrid functionals used have a different amount of the exact exchange (ranging from 10% in TPSSh to 54% in M06-2X). All open-shell systems are treated with unrestricted formalism. Broken symmetry solutions are obtained from the high spin states with the spin-flip method. All calculations were performed with an increased numerical integration grid ("quality good" in ADF).

The nature of the metal-ligand bonding was analyzed with the Extended Transition State Energy Decomposition scheme (EDA) [37–39]. The interaction energy, E_{int}, between chosen fragments is decomposed into three chemically significant components i) the quasi-classical electrostatic interaction between the fragments (E_{elst}); ii) the repulsive Pauli interaction (E_{Pauli}); iii) the orbital stabilizing contribution due to the covalency, i.e., charge transfer, and polarization (E_{orb}). In addition to the E_{int}, the preparation energy E_{prep}, the energy required to bring separated fragments from their equilibrium geometry to the geometry they adopt in complex ions, is considered. Furthermore, natural orbitals for chemical valence (NOCV)[40, 41] decomposition of the electron density deformation was performed to elucidate different density transfer channels and to quantify their importance as an energy contribution to the E_{orb}. Charge flow between the fragments was quantified with the Hirshfeld charge analysis[65]. For $[Fe(CO)_4]^{2-}$ the interaction between $[Fe(CO)_3]^{2-}$ and CO was analyzed. For $[Fe(CO)_3(NO)]^{-}$ three possibilities were considered: i) interaction between closed-shell $[Fe(CO)_3]^{2-}$ and NO^+ ii) interaction between $[Fe(CO)_3]^{-}$ and NO iii) interaction between $[Fe(CO)_3]$ and NO^{-}. In cases ii) and iii), spin-unrestricted fragments were used. $[Fe(CO)_3]^{-}$ and NO fragments are considered in doublet states, while $[Fe(CO)_3]$ and NO^{-} fragments in triplet states.

3. Results and Discussion

As we stated in the Introduction, determination of the spin ground state with DFT is a delicate task, and strongly depend on the choice of the DFA. Therefore, we examined 12 different functionals (GGAs, meta-GGAs, hybrid functionals, as well as long-range, and meta-hybrid functionals) and their performance on the spin ground state for both complexes under study (Table 1). GGA and meta-GGA functionals always give closed-shell singlet as the ground state, with triplet higher in energy. The performance of hybrid and meta-hybrid functionals depends on the percentage of the exact HF exchange. The high spin states are more stabilized as the percentage of the exact exchange is higher. The closed-shell singlet state is still the ground state with functionals having low (TPSSh with 10%, B3LYP* with 15%) to moderate (B3LYP with 20%, M06 with 27%) amount of the HF exchange. BHandHLYP and M06-2X favor the broken symmetry solution. This is due to a large amount of the exact exchange (50% in BHandHLYP, and 54% in M06-2X) leading to the artificial symmetry breaking [6, 66]. The most reasonable results have been obtained with long-range separated hybrid CAMY-B3LYP: the ground state of $[Fe(CO)_4]^{2-}$ is a closed-shell singlet

with a broken symmetry singlet state approx. 70 kcal/mol higher in energy, in accordance with previous findings [11, 12], while in the case of $[Fe(CO)_3(NO)]^-$ closed-shell singlet and open-shell singlet are similar in energy, later being more stable for 0.8 kcal/mol.

Table 1 Spin-state energy differences in $[Fe(CO)_4]^{2-}$ and $[Fe(CO)_3(NO)]^-$ with different DFAs at X-ray geometries (CCDC 1217933 [11], 1266312 [50]); energies are given in kcal/mol relative to the closed-shell singlet states.

	$[Fe(CO)_4]^{2-}$			$[Fe(CO)_3NO]^-$		
GGA	BP86-D4		OPBE	BP86-D4		OPBE
Singlet	0.00		0.00	0.00		0.00
Triplet	73.01		77.79	56.43		55.66
Quintet	152.89		155.41	110.24		105.75
Open-shell Singlet	73.82[a]		79.24[a]	65.69[a]		65.86[a]
Meta-GGA	M06-L	TPSS	SCAN	M06-L	TPSS	SCAN
Singlet	0	0	0	0	0	0
Triplet	81.09	76.22	74.27	53.28	54.49	49.85
Quintet	155.09	154.83	148.9	98.51	106.18	94.15
Open-shell Singlet	86.30[a]	77.03[a]	76.51[a]	64.43[a]	64.41[a]	61.07[a]
Hybrid	B3LYP*	B3LYP	BHandHLYP	B3LYP*	B3LYP	BHandHLYP
Singlet	0	0.00	0.00	0	0.00	0.00
Triplet	69.10	67.55	57.57	48.14	44.54	23.31
Quintet	145.06	141.4	115.03	93.16	85.73	39.73
Open-shell Singlet	69.56[a]	68.67[a]	-1.9	65.28[a]	56.23[a]	-17.95
Meta-Hybrid	TPSSh	M06	M06-2X	TPSSh	M06	M06-2X
Singlet	0	0	0	0	0	0
Triplet	74.63	75.92	50.17	48.69	46.53	18.33
Quintet	149.75	147.13	107.06	94.18	86.2	40.13
Open-shell Singlet	77.03[a]	75.12[a]	-3.33	64.66[a]	64.90[a]	-18.06[a]
Long-range	CAMY-B3LYP			CAMY-B3LYP		
Singlet	0.00			0.00		
Triplet	68.94			40.57		
Quintet	141.26			78.82		
Open-shell Singlet	69.33[a]			-0.84		

[a] "non-*aufbau*" occupation of KS-MOs

EDA analysis with CAMY-B3LYP provides insight into the nature of the Fe-CO bond (Table 2). The attractive interactions (E_{elst} and E_{orb}) are the indications of ionic vs. covalent bonding, respectively. It is clear from Table 2 that Fe-CO bonding can be described as 50% ionic and 50% covalent in line with transfer of charge from $[Fe(CO)_3]^{2-}$ fragment to CO. The same picture is obtained with other DFA's (Table S1 in SI).

Table 2 Energy Decomposition Analysis of $[Fe(CO)_3]^{2-}$-- CO at SR-ZORA-CAMY-B3LYP/TZP level of theory; energy components are given in kcal/mol relative to the chosen fragments; ΔQ is Hirshfeld charge, transferred between fragments; $E = E_{int} + E_{prep}$.

	E_{Pauli}	E_{elst}	E_{orb}	E_{int}	E_{prep}	E	ΔQ
$[Fe(CO)_3]^{2-}$-- CO	121.79	-104.05	-102.62	-84.88	14.42	-70.46	0.45[a]

[a] charge is transferred from $[Fe(CO)_3]^{2-}$ fragment to CO fragment

NOCV scheme reveals three dominant electron density flow channels and clarifies the covalent character of the bonding, Fig. 1. The most important contribution is π*-back-donation from Fe d-orbitals (Fig. 1a and Fig. 1b). The π*-accepting properties of coordinated ligands are crucial for bonding in d^{10} complexes [43]. Another important contribution is σ-donation from the lone pair of CO ligand and the charge accumulation in the bonding region (Fig. 1c). The other contributions are mainly polarization because of small Hirshfeld charge transfer, Δq, indicating the intra-fragment character of density transfers.

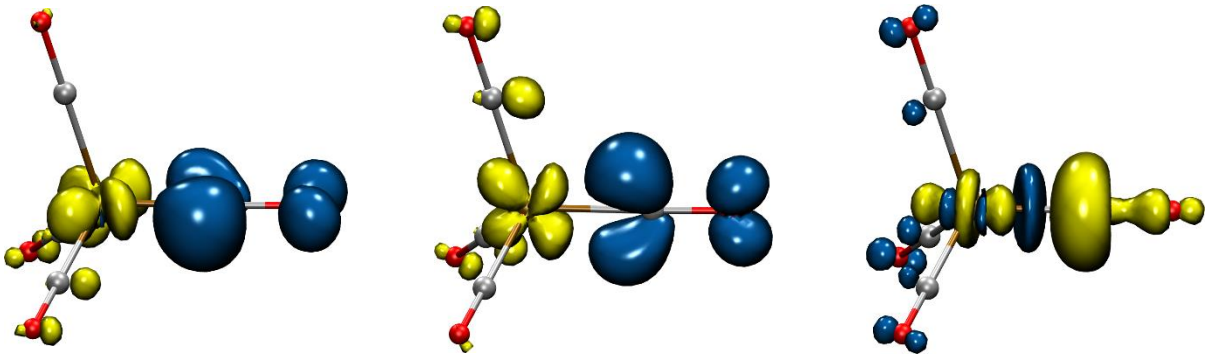

a) *E*= -38 kcal/mol; Δq=0.29

b) *E*= -36 kcal/mol; Δq=0.28

c) *E*= -18 kcal/mol; Δq=0.16

Fig. 1 Most important density deformation channels from EDA-NOCV analysis of $[Fe(CO)_3]^{2-}$-- CO interaction: a) and b) π*-back-donation c) σ -Fe-CO bond. Their relevance is given by their energy contribution E to E_{orb} and by Hirshfeld charge transferred between the fragments Δq. Charge outflow/inflow is represented by yellow/blue color (isovalue=0.005 a.u.)

Calculations on $[Fe(CO)_3(NO)]^{-}$ were performed considering different oxidation state of the central Fe atom and the resulting charge of the nitric oxide: i) Fe(-II) (d^{10} electronic configuration) and NO^+, giving closed-shell singlet as the ground state; ii) Fe(-I) and NO, with one unpaired electron on the iron center (d^9 electronic configuration) and one unpaired electron on the neutral nitrosyl ligand giving open-shell singlet as the ground state; iii) Fe(0) and NO^- with two unpaired electrons on both centers, leading to the open-shell singlet state, as the ground state. Because of the covalent character of bonding with nitrosyl ligand, the open-shell singlet states prepared as in ii) and iii), according to our calculations, converge to

the same electronic distribution. It has been previously shown [6, 7], and our calculations proved it, that determination of the ground state is influenced by the chosen DFA (Table 1). High spin states (triplet in the case ii) and quintet in the case iii)) are always much higher in energy. Looking only at the ground state energies will not give an unambiguous conclusion on the electronic structure. Therefore, we performed EDA analysis with a different selection of fragments, i.e., choices i), ii), and iii), Table 3. To compare three different decisions, energy E_{rel} is stated as the energy difference relative to the most stable relaxed fragment pairs ($[Fe(CO)_3]^-$/NO).

Table 3 Energy Decomposition Analysis of $[Fe(CO)_3$--$NO]^-$ for different fragmentation patterns, i), ii) and iii) at SR-ZORA-CAMY-B3LYP/TZP level of theory; energy components are given in kcal/mol relative to the chosen fragments; $E_{rel}=E_{int}+E_{prep}$ relative to the relaxed $[Fe(CO)_3]^-$/NO pair; ΔQ is Hirshfeld charge, transferred between fragments.

		E_{Pauli}	E_{elst}	E_{orb}	E_{int}	E_{prep}	E_{rel}	ΔQ
i)	$[Fe(CO)_3]^{2-}$--NO^+	105.95	-210.78	-324.34	-447.17	86.07	-65.17	1.25[a]
ii)	$^2[Fe(CO)_3]^-$-- ^2NO	160.12	-93.37	-156.68	-89.94	23.95	-65.99	0.46[b]
iii)	$^3[Fe(CO)_3]$ -- $^3NO^-$	195.04	-178.47	-122.76	-106.19	4.22	-65.99	0.28[c]

i) closed-shell singlet $[Fe(CO)_3NO]^-$ ii) and iii) open-shell singlet $[Fe(CO)_3$-$NO]^-$

[a] charge is transferred from $[Fe(CO)_3]^{2-}$ fragment to NO^+ fragment

[b] charge is transferred from $[Fe(CO)_3]^-$ fragment to NO fragment

[c] charge is transferred from NO^- fragment to $[Fe(CO)_3]$

Energy differences between three possible fragmentation choices are small and in line with DFT calculations, showing that the broken-symmetry solution is more stable for approx. 0.8 kcal/mol. However, energy components are entirely different, indicating the importance of the fragment choice. Different fragment alternatives reflect the diverse nature of the interaction between fragments. The model, which is the closest to the physical reality, is the one with the lowest absolute value of E_{orb} [67]. Orbital interaction takes into account the significance of the charge transfer between the fragments. Thus, $[Fe(CO)_3]$--NO^- choice of fragments, iii), is the most similar to the final electronic structure of the complex anion, Table 3. Moreover, in the situation i) ΔQ is very large, showing a tendency to reduce NO^+. It is noteworthy that even different DFAs, that give different ground states, in EDA analysis give the same trends (Tables S2 and S3 in Supplementary material).

NOCV analysis for the first fragmentation scheme reveals almost exclusive π*-back-donation to the NO^+ (Fig. 2a and Fig. 2b). These two, most dominant electron density flows contribute more than 90% to E_{orb} and include the transfer of 1.4 electrons, oxidize iron, and suggest that iron cannot be in the -II oxidation state, supplementing previous arguments. The third density flow channel is clear σ-donation but is of minor importance (Fig. 2c). The same analysis on the broken symmetry $[Fe(CO)_3]$--NO^- also shows the importance of π bonding between the fragments (Fig. 3). Four most dominant density flow channels correspond to the α-π*-back-donation (Fig. 3a and Fig. 3b) and β-π*-donation (Fig. 3c and Fig. 3d). σ-type interaction

between the fragments (Fig. 3e) contributes around 27% to the E_{orb}, but a minimal amount of charge is transferred between the fragments (0.09 electrons).

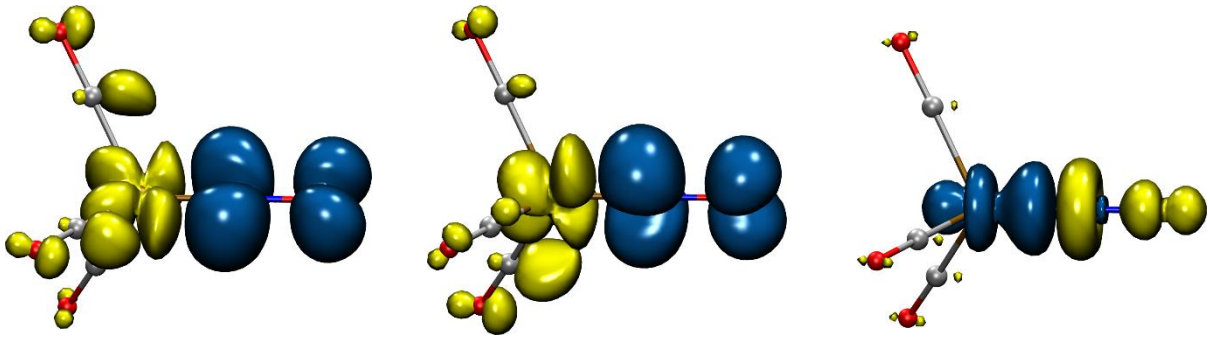

a) *E* = -149 kcal/mol; Δq=0.72

b) *E* = -149 kcal/mol; Δq=0.72

c) *E* = -17 kcal/mol; Δq=0.14

Fig 2 Most important density deformation channels from EDA-NOCV analysis of $[Fe(CO)_3]^{2-}$-- NO^+ interaction: a) and b) π*-back-donation c) σ-donation. Their relevance is given by their energy contribution *E* to E_{orb} and by Hirshfeld charge transferred between the fragments Δq. Charge outflow/inflow is represented by yellow/blue color (isovalue=0.005 a.u.)

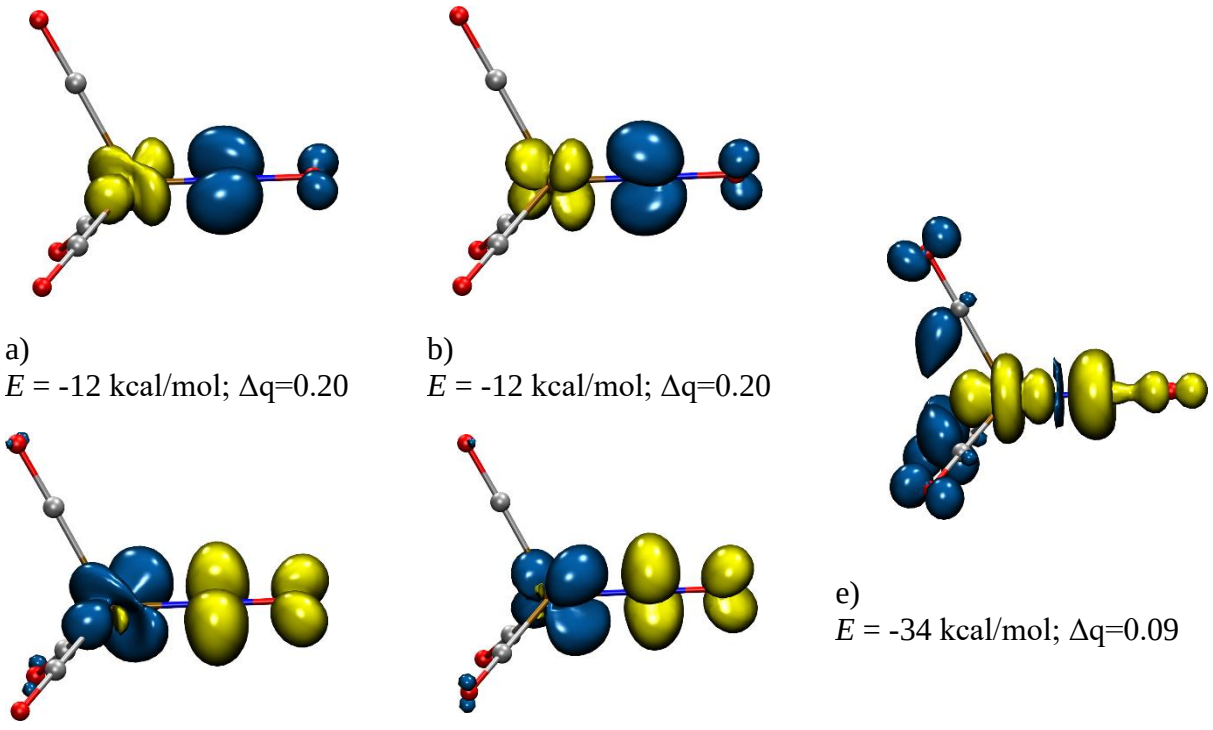

a) *E* = -12 kcal/mol; Δq=0.20

b) *E* = -12 kcal/mol; Δq=0.20

e) *E* = -34 kcal/mol; Δq=0.09

c) *E* = -22 kcal/mol; Δq=0.31

d) *E* = -22 kcal/mol; Δq=0.31

Fig 3 Most important density deformation channels from EDA-NOCV analysis of $[Fe(CO)_3]$-- NO^- interaction: a) and b) α-π*-back-donation c) and d) β-π*-donation e) σ-polarization. Their relevance is given by their energy contribution *E* to E_{orb} and by Hirshfeld charge transferred between the

fragments Δq. Charge outflow/inflow is represented by yellow/blue color (isovalue=0.005 a.u. in a), b, c), d) and isovalue= 0.0025 a.u. in e))

4. Conclusions

With the approach of combined Energy Decomposition Analysis and Natural Orbital for Chemical Valence, new insights into the electronic structure of the $[Fe(CO)_3(NO)]^-$ has been gained. The results are also compared with the $[Fe(CO)_4]^{2-}$, where iron is in the formal oxidation state -II. DFT calculations did not give an obvious conclusion about the oxidation state of the iron atom and the resulting charge of the nitric oxide ligand. The computed ground state depends on the chosen functional. With GGA, meta-GGA, hybrid and meta-hybrid functionals with a lower percentage of the exact exchange, the electronic structure of $[Fe(CO)_3(NO)]^-$ correspond to the $[Fe(CO)_4]^{2-}$, i.e., Fe(-II) (d^{10} electronic configuration) and NO^+. On the other hand, hybrid and meta-hybrid functionals with a higher percentage of the exact exchange (e.g., BHandHLYP and M06-2X), as well as long-range separated CAMY-B3LYP gave the open-shell singlet with Fe(0) and NO^-.

However, it has been shown that the trends in EDA are irrespective of the chosen functional. The choice of fragments in EDA is a clear indication of actual bonding in analyzed complexes. The orbital contribution is an indicator of how well the chosen fragments represent the real picture. The lowest absolute value of E_{orb} suggests that the electronic state of $[Fe(CO)_3(NO)]^-$ is the best described with iron in zero formal oxidation state bounded to the nitrosyl anion. Furthermore, NOCV analysis on $[Fe(CO)_3]^{2-}$--NO^+ fragments show large charge flow from iron to NO^+ ligand, confirming that iron cannot be in –II oxidation state. Comparison with its analog $[Fe(CO)_4]^{2-}$ showed that the nature of bonding is different.

References

1. Chan WTK, Wong WT (2013) A brief introduction to transition metals in unusual oxidation states. Polyhedron 52:43–61. https://doi.org/10.1016/j.poly.2012.09.004
2. Ellis JE (2006) Adventures with Substances Containing Metals in Negative Oxidation States. Inorg Chem 45:3167–3186. https://doi.org/10.1021/ic052110i
3. Allan M, Lacko M, Papp P, Matejčík Š, Zlatar M, Fabrikant II, Kočišek J, Fedor J (2018) Dissociative electron attachment and electronic excitation in Fe(CO)5. Phys Chem Chem Phys 20:11692–11701. https://doi.org/10.1039/C8CP01387J
4. Ellis JE (2003) Metal Carbonyl Anions: from [Fe(CO)4]2- to [Hf(CO)6]2- and Beyond. Organometallics 22:3322–3338. https://doi.org/10.1021/om030105l
5. Plietker B, Dieskau A (2009) The Reincarnation of the Hieber Anion [Fe(CO)3(NO)]- - a New Venue in Nucleophilic Metal Catalysis. European J Org Chem 2009:775–787. https://doi.org/10.1002/ejoc.200800893
6. Klein JEMN, Miehlich B, Holzwarth MS, Bauer M, Milek M, Khusniyarov MM, Knizia G, Werner H-J, Plietker B (2014) The Electronic Ground State of [Fe(CO)3(NO)]− : A Spectroscopic and Theoretical Study. Angew Chemie Int Ed 53:1790–1794. https://doi.org/10.1002/anie.201309767
7. Burkhardt L, Vukadinovic Y, Nowakowski M, Kalinko A, Rudolph J, Carlsson P-A, Jacob

CR, Bauer M (2020) Electronic Structure of the Hieber Anion [Fe(CO)3(NO)]− Revisited by X-ray Emission and Absorption Spectroscopy. Inorg Chem 59:3551–3561. https://doi.org/10.1021/acs.inorgchem.9b02092
8. Klein JEMN, Knizia G, Miehlich B, Kästner J, Plietker B (2014) Fe or Fe-NO Catalysis? A Quantum Chemical Investigation of the [Fe(CO)3(NO)]− - Catalyzed Cloke-Wilson Rearrangement. Chem - A Eur J 20:7254–7257. https://doi.org/10.1002/chem.201402716
9. Weisser F, Klein JEMN, Sarkar B, Plietker B (2014) Spectroelectrochemical investigation of Bu4N[Fe(CO)3(NO)]: identification of a reversible EC-mechanism. Dalt Trans 43:883–887. https://doi.org/10.1039/C3DT51998H
10. Klein J (2011) The Hieber Anion [Fe(CO)3(NO)]-. Synlett 2011:2757–2758. https://doi.org/10.1055/s-0031-1289559
11. Teller RG, Finke RG, Collman JP, Chin HB, Bau R (1977) Dependence of the tetracarbonylferrate(2-) geometry on counterion: crystal structures of dipotassium tetracarbonylferrate and bis(sodium crypt) tetracarbonylferrate [crypt = N(CH2CH2OCH2CH2OCH2CH2)3N]. J Am Chem Soc 99:1104–1111. https://doi.org/10.1021/ja00446a022
12. Collman JP (1975) Disodium tetracarbonylferrate, a transition metal analog of a Grignard reagent. Acc Chem Res 8:342–347. https://doi.org/10.1021/ar50094a004
13. Cramer CJ, Truhlar DG (2009) Density functional theory for transition metals and transition metal chemistry. Phys Chem Chem Phys 11:10757. https://doi.org/10.1039/b907148b
14. Zlatar M, Gruden M (2020) Introduction to ligand field theory and computational chemistry. In: Crichton RR, Louro RO (eds) Practical Approaches to Biological Inorganic Chemistry, 2nd ed. Elsevier, pp 17–67
15. Singh SK, Eng J, Atanasov M, Neese F (2017) Covalency and chemical bonding in transition metal complexes: An ab initio based ligand field perspective. Coord Chem Rev 344:2–25. https://doi.org/10.1016/j.ccr.2017.03.018
16. Reiher M (2009) A Theoretical Challenge: Transition-Metal Compounds. Chimia (Aarau) 63:140–145. https://doi.org/10.2533/chimia.2009.140
17. Jørgensen CK (1966) Differences between the four halide ligands, and discussion remarks on trigonal-bipyramidal complexes, on oxidation states, and on diagonal elements of one-electron energy. Coord Chem Rev 1:164–178. https://doi.org/10.1016/S0010-8545(00)80170-8
18. Enemark JH, Feltham RD (1974) Principles of structure, bonding, and reactivity for metal nitrosyl complexes. Coord Chem Rev 13:339–406. https://doi.org/10.1016/S0010-8545(00)80259-3
19. Kaim W, Das A, Fiedler J, Záliš S, Sarkar B (2020) NO and NO2 as non-innocent ligands: A comparison. Coord Chem Rev 404:213114. https://doi.org/10.1016/j.ccr.2019.213114
20. Ye S, Neese F (2010) The Unusual Electronic Structure of Dinitrosyl Iron Complexes. J Am Chem Soc 132:3646–3647. https://doi.org/10.1021/ja9091616
21. Monsch G, Klüfers P (2019) [Fe(H2O)5(NO)]2+, the “Brown-Ring” Chromophore. Angew Chemie Int Ed 58:8566–8571. https://doi.org/10.1002/anie.201902374
22. Boulet P, Buchs M, Chermette H, Daul C, Gilardoni F, Rogemond F, Schläpfer CW, Weber J (2001) DFT Investigation of Metal Complexes Containing a Nitrosyl Ligand. 1. Ground State and Metastable States. J Phys Chem A 105:8991–8998. https://doi.org/10.1021/jp010988z
23. Boulet P, Buchs M, Chermette H, Daul C, Furet E, Gilardoni F, Rogemond F, Schläpfer CW, Weber J (2001) DFT Investigation of Metal Complexes Containing a Nitrosyl Ligand. 2. Excited States. J Phys Chem A 105:8999–9003. https://doi.org/10.1021/jp010989r
24. Noodleman L (1981) Valence bond description of antiferromagnetic coupling in transition metal dimers. J Chem Phys 74:5737–5743. https://doi.org/10.1063/1.440939
25. Noodleman L, Davidson ER (1986) Ligand spin polarization and antiferromagnetic coupling in transition metal dimers. Chem Phys 109:131–143. https://doi.org/10.1016/0301-0104(86)80192-6
26. Neese F (2009) Prediction of molecular properties and molecular spectroscopy with density functional theory: From fundamental theory to exchange-coupling. Coord Chem Rev 253:526–563. https://doi.org/10.1016/j.ccr.2008.05.014
27. Zhang Y, Yang W (1998) A challenge for density functionals: Self-interaction error increases

for systems with a noninteger number of electrons. J Chem Phys 109:2604–2608. https://doi.org/10.1063/1.476859
28. Parthey M, Kaupp M (2014) Quantum-chemical insights into mixed-valence systems: within and beyond the Robin–Day scheme. Chem Soc Rev 43:5067–5088. https://doi.org/10.1039/C3CS60481K
29. Bally T, Sastry GN (1997) Incorrect Dissociation Behavior of Radical Ions in Density Functional Calculations. J Phys Chem A 101:7923–7925. https://doi.org/10.1021/jp972378y
30. Chermette H, Ciofini I, Mariotti F, Daul C (2001) Correct dissociation behavior of radical ions such as H2+ in density functional calculations. J Chem Phys 114:1447–1453. https://doi.org/10.1063/1.1332989
31. Dreuw A, Head-Gordon M (2004) Failure of Time-Dependent Density Functional Theory for Long-Range Charge-Transfer Excited States: The Zincbacteriochlorin−Bacteriochlorin and Bacteriochlorophyll−Spheroidene Complexes. J Am Chem Soc 126:4007–4016. https://doi.org/10.1021/ja039556n
32. Gerber IC, Ángyán JG (2005) Hybrid functional with separated range. Chem Phys Lett 415:100–105. https://doi.org/10.1016/j.cplett.2005.08.060
33. Vydrov OA, Scuseria GE (2006) Assessment of a long-range corrected hybrid functional. J Chem Phys 125:234109. https://doi.org/10.1063/1.2409292
34. Renz M, Theilacker K, Lambert C, Kaupp M (2009) A Reliable Quantum-Chemical Protocol for the Characterization of Organic Mixed-Valence Compounds. J Am Chem Soc 131:16292–16302. https://doi.org/10.1021/ja9070859
35. Kaduk B, Kowalczyk T, Van Voorhis T (2012) Constrained Density Functional Theory. Chem Rev 112:321–370. https://doi.org/10.1021/cr200148b
36. Daul C (1994) Density functional theory applied to the excited states of coordination compounds. Int J Quantum Chem 52:867–877. https://doi.org/10.1002/qua.560520414
37. Ziegler T, Rauk A (1977) On the calculation of bonding energies by the Hartree Fock Slater method. Theor Chim Acta 46:1–10. https://doi.org/10.1007/BF02401406
38. Ziegler T, Rauk A (1979) A theoretical study of the ethylene-metal bond in complexes between copper(1+), silver(1+), gold(1+), platinum(0) or platinum(2+) and ethylene, based on the Hartree-Fock-Slater transition-state method. Inorg Chem 18:1558–1565. https://doi.org/10.1021/ic50196a034
39. Bickelhaupt FM, Baerends EJ (2000) Kohn-Sham Density Functional Theory: Predicting and Understanding Chemistry. In: Lipkowitz KB, Boyd DB (eds) Reviews in computational chemistry. Wiley-VCH Verlag, pp 1–86
40. Nalewajski RF, Mrozek J, Mazur G (1996) Quantum chemical valence indices from the one-determinantal difference approach. Can J Chem 74:1121–1130. https://doi.org/10.1139/v96-126
41. Mitoraj MP, Michalak A, Ziegler T (2009) A Combined Charge and Energy Decomposition Scheme for Bond Analysis. J Chem Theory Comput 5:962–975. https://doi.org/10.1021/ct800503d
42. Vujović M, Zlatar M, Milčić M, Gruden M (2017) in/out Isomerism of cyclophanes: a theoretical account of 2,6,15-trithia-[3 4,10][7]metacyclophane and [3 4,10][7]metacyclophane as well as their halogen substituted analogues. Phys Chem Chem Phys 19:9500–9508. https://doi.org/10.1039/C7CP00557A
43. Zlatar M, Allan M, Fedor J (2016) Excited States of Pt(PF3)4 and Their Role in Focused Electron Beam Nanofabrication. J Phys Chem C 120:10667–10674. https://doi.org/10.1021/acs.jpcc.6b02660
44. Vermeeren P, van der Lubbe SCC, Fonseca Guerra C, Bickelhaupt FM, Hamlin TA (2020) Understanding chemical reactivity using the activation strain model. Nat Protoc 15:649–667. https://doi.org/10.1038/s41596-019-0265-0
45. Wu X, Zhao L, Jin J, Pan S, Li W, Jin X, Wang G, Zhou M, Frenking G (2018) Observation of alkaline earth complexes M(CO)8 (M = Ca, Sr, or Ba) that mimic transition metals. Science (80-) 361:912–916. https://doi.org/10.1126/science.aau0839
46. Baerends EJ, Ziegler T, Atkins AJ, et al ADF2017, SCM, Theoretical Chemistry, Vrije Universiteit, Amsterdam, The Netherlands, https://www.scm.com

47. te Velde G, Bickelhaupt FM, Baerends EJ, Fonseca Guerra C, van Gisbergen SJA, Snijders JG, Ziegler T (2001) Chemistry with ADF. J Comput Chem 22:931–967. https://doi.org/10.1002/jcc.1056
48. Guerra CF, Snijders JG, te Velde G, Baerends EJ (1998) Towards an order-N DFT method. Theor Chem Acc 99:391–403
49. Lenthe E van, Baerends EJ, Snijders JG (1993) Relativistic regular two-component Hamiltonians. J Chem Phys 99:4597–4610. https://doi.org/10.1063/1.466059
50. Clarkson LM, Clegg W, Hockless DCR, Norman NC (1992) Structure of a thallium(I) transition-metal carbonyl salt Tl[Fe(CO)3(NO)]. Acta Crystallogr Sect C Cryst Struct Commun 48:236–239. https://doi.org/10.1107/s0108270191010405
51. Seth M, Ziegler T (2012) Range-separated exchange functionals with Slater-type functions. J Chem Theory Comput 8:901–907. https://doi.org/10.1021/ct300006h
52. Akinaga Y, Ten-no S (2008) Range-separation by the Yukawa potential in long-range corrected density functional theory with Gaussian-type basis functions. Chem Phys Lett 462:348–351. https://doi.org/10.1016/j.cplett.2008.07.103
53. Yanai T, Tew DP, Handy NC (2004) A new hybrid exchange-correlation functional using the Coulomb-attenuating method (CAM-B3LYP). Chem Phys Lett 393:51–57. https://doi.org/10.1016/j.cplett.2004.06.011
54. Becke AD (1988) Density-functional exchange-energy approximation with correct asymptotic behavior. Phys Rev A 38:3098–3100. https://doi.org/10.1103/PhysRevA.38.3098
55. Perdew JP (1986) Density-functional approximation for the correlation energy of the inhomogeneous electron gas. Phys Rev B 33:8822–8824. https://doi.org/10.1103/PhysRevB.33.8822
56. Perdew JP (1986) Erratum: Density-functional approximation for the correlation energy of the inhomogeneous electron gas. Phys Rev B 34:7406–7406. https://doi.org/10.1103/PhysRevB.34.7406
57. Swart M, Ehlers AW, Lammertsma K (2004) Performance of the OPBE exchange-correlation functional. Mol Phys 102:2467–2474. https://doi.org/10.1080/00268970420002750l7
58. Zhao Y, Truhlar DG (2006) A new local density functional for main-group thermochemistry, transition metal bonding, thermochemical kinetics, and noncovalent interactions. J Chem Phys 125:194101. https://doi.org/10.1063/1.2370993
59. Zhao Y, Truhlar DG (2008) The M06 suite of density functionals for main group thermochemistry, thermochemical kinetics, noncovalent interactions, excited states, and transition elements: two new functionals and systematic testing of four M06-class functionals and 12 other function. Theor Chem Acc 120:215–241. https://doi.org/10.1007/s00214-007-0310-x
60. Tao J, Perdew J, Staroverov V, Scuseria G (2003) Climbing the Density Functional Ladder: Nonempirical Meta–Generalized Gradient Approximation Designed for Molecules and Solids. Phys Rev Lett 91:146401. https://doi.org/10.1103/PhysRevLett.91.146401
61. Staroverov VN, Scuseria GE, Tao J, Perdew JP (2003) Comparative assessment of a new nonempirical density functional: Molecules and hydrogen-bonded complexes. J Chem Phys 119:12129. https://doi.org/10.1063/1.1626543
62. Sun J, Ruzsinszky A, Perdew J (2015) Strongly Constrained and Appropriately Normed Semilocal Density Functional. Phys Rev Lett 115:036402. https://doi.org/10.1103/PhysRevLett.115.036402
63. Reiher M, Salomon O, Artur Hess B (2001) Reparameterization of hybrid functionals based on energy differences of states of different multiplicity. Theor Chem Accounts Theory, Comput Model (Theoretica Chim Acta) 107:48–55. https://doi.org/10.1007/s00214-001-0300-3
64. Stephens PJ, Devlin FJ, Chabalowski CF, Frisch MJ (1994) Ab Initio Calculation of Vibrational Absorption and Circular Dichroism Spectra Using Density Functional Force Fields. J Phys Chem 98:11623–11627. https://doi.org/10.1021/j100096a001
65. Hirshfeld FL (1977) Bonded-atom fragments for describing molecular charge densities. Theor Chim Acta 44:129–138. https://doi.org/10.1007/BF00549096
66. Sherrill CD, Lee MS, Head-Gordon M (1999) On the performance of density functional theory for symmetry-breaking problems. Chem Phys Lett 302:425–430.

https://doi.org/10.1016/S0009-2614(99)00206-7
67. Scharf LT, Andrada DM, Frenking G, Gessner VH (2017) The Bonding Situation in Metalated Ylides. Chem - A Eur J 23:4422–4434. https://doi.org/10.1002/chem.201605997